JOURNAL OF PROPULSION AND POWER
Vol. 17, No. 6, November–December 2001

Development Study of a Precooler for the Air-Turboramjet Expander-Cycle Engine

Kenya Harada*
National Aerospace Laboratory, Chofu, Tokyo 182-8522, Japan
and
Nobuhiro Tanatsugu† and Tetsuya Sato‡
Institute of Space and Astronautical Science, Sagamihara, Kanagawa 229-8510, Japan

A review of the development of a precooler for the air-turboramjet expander-cycle (ATREX) engine is given. Three types of precooler for the ATREX engine ground-test model were designed, manufactured, and tested under sea-level static conditions. The results suggested two problems affecting the precooler performance, heat transfer rate and airflow pressure drop. One is nonuniformity of the airflow through the tube banks. The other problem is frost formation on the heat transfer surfaces. Concerning nonuniformity of airflow, the shell configuration was modified based on analysis by computational fluid dynamics calculation. To improve the precooler performance under frosting condition, a new method to add a condensable gas into the airflow was proposed and examined by experiments on a subscale heat exchanger model. Addition of a small quantity of ethanol can effectively restrain the decline of the precooler performance due to frost formation.

Introduction

THE air-turboramjet engine with expander cycle (ATREX engine) has been under development since 1986.[1] The ATREX engine is intended as the propulsion system for a fly-back booster up to Mach 6 at an altitude of 30 km of a reusable two-stage-to-orbit space plane. Figure 1 shows a flow diagram of the ATREX engine.

One of the key components of the ATREX engine is the precooler, which is a heat exchanger to cool the incoming air in front of the fan by using the hydrogen fuel as a coolant. Precooling air gives the following benefits: increase of flight allowable Mach number, increase of thrust, and increase of specific impulse. However, these benefits are offset by additional pressure drop of the airflow and by increase of the engine size and mass. These facts strongly demand the development of compact and lightweight heat exchangers with high heat transfer rate and low pressure drop. An additional problem is the frost formation on the heat transfer surfaces. It induces even more pressure drop and reduces heat transfer rate. In very unfavorable cases it may even choke the airflow.

Review of Precooler Development

Figure 2 shows the timescale of the precooler development. Elementary tests with subscale heat exchangers from 1992 to 1994 investigated the characteristics of heat transfer rate and pressure drop using various configurations of heat transfer surfaces, such as circular tube banks, elliptic tube banks, and those with fins. Since 1995, three models of precooler (called type I, II, and III) have been designed and manufactured for the ATREX engine ground-test model. The configurations of the models are shown in Figs. 3–5, and their characteristics are listed in Table 1. They are all shell-and-tube-type heat exchangers consisting of circular tubes arranged in annular, as shown in Fig. 6. These tubes are grouped with eight (type I) or six (types II and III) paths with several rows in the radial direction. These paths are connected in series. Coolant flows from the inner to the outer paths, changing its flow direction. The incoming air flows through tube banks from outside to inside passing three (type I) or five (types II and III) sections, which are divided by tube supporting plates at an angle of 70 (type I) or 90 (types II and III) deg to the tubes.

Type-I Model

A number of configurations of precooler were examined analytically and the final configuration of type-I model was selected by Balepin.[2] This model was installed into the ATREX engine and tested under the sea-level static conditions.[3,4] This was the first experience of a precooled cycle engine firing test, to the best of our knowledge. After four test runs (250 s) some leakage of coolant occurred at the brazing points because of fatigue failure due to vibration from the turbomachinery. However, the hydraulic and thermal characteristics of the precooler model and its effect on the engine performance were investigated.

The airflow was cooled down to 180 K by the precooler; consequently, the engine thrust and the specific impulse were increased by 80 and 25%, respectively.[3] However, the actual heat transfer rates were 15–20% smaller than predicted, which was caused by the following effects: thermal resistance of the frost layer formed on the tube surface and nonuniformity of the airflow through the tube banks.

Frost formation on the tube surface was observed from the beginning of cooling in all tests, as shown in Fig. 7. However, the frost layer was so thin compared with the tube gap that almost no additional pressure drop due to the frost formation resulted during the test. On the other hand, computational fluid dynamics analysis of the airflow in the precooler shell made it clear that severe nonuniformity of the airflow followed by an additional pressure drop was caused by the steep expansion of the flow area at the inlet part.

Type-II Model

The type-II model is similar to type I, but some modifications were done for the following objectives[4]: to improve reliability and durability and to reduce air pressure drop due to the shell configuration.

To achieve the first objective, large-diameter tubes were used at some cost in performance. These tubes were bent at the front end of the tube assembly to reduce the brazing points. The supporting

Presented as Paper 99-4897 at the 9th International Space Planes and Hypersonic Systems and Technologies Conference, Norfolk, VA, 1–5 November 1999; received 23 July 2000; revision received 15 December 2000; accepted for publication 29 December 2000.

*Researcher, Fluid Science Research Center, 7-44-1 Jindaiji-Higashi; kenya@nal.go.jp. Member AIAA.
†Professor, Space Propulsion System Division, 3-1-1, Yoshinodai. Member AIAA.
‡Research Associate, Space Propulsion System Division, 3-1-1, Yoshinodai. Member AIAA.

Table 1 Precooler models characteristics

Characteristic	Type I	Type II	Type III
Tube outer diameter, mm	3	5	2
Tube wall thickness, mm	0.15	0.3	0.15
Tube length, mm	820	820	525
Number of tube rows			
in circumferential direction	280	176	376/436/524[a]
in radial direction	24	18	4/5/6[a]
Total number of tubes	6,720	3,168[b]	13,464[b]
Heat transfer area, m^2	51.9	40.8	44.4
Volume of tube banks, m^3	0.154	0.154	0.080
Compactness, m^2/m^3	338	265	553
Total weight of unit, kg	300	350	160
Number of transfer units[c]	3.11	2.03	3.89

[a] Coolant first and second/third and fourth/fifth and sixth path.
[b] Each U-shape tube counts as 2 tubes.
[c] Design value for 8 kg/s of airflow.

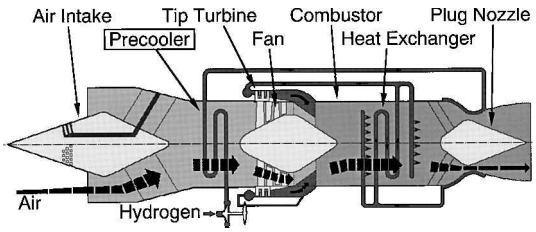

Fig. 1 Flow diagram of ATREX engine.

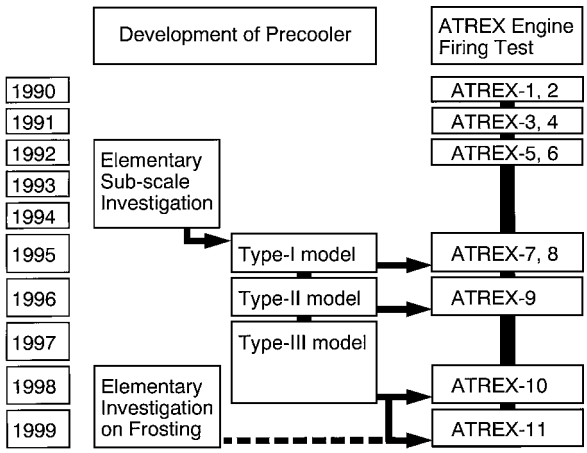

Fig. 2 History of precooler development.

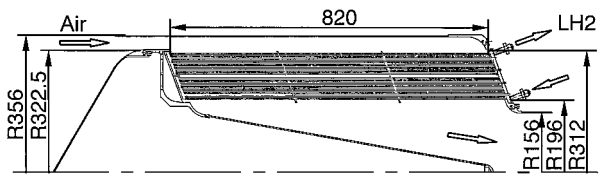

Fig. 3 Configuration of type-I model.

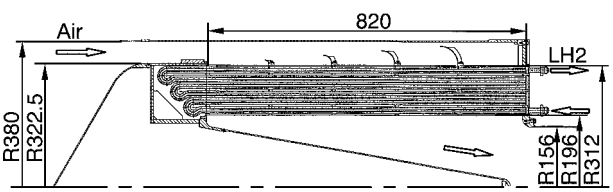

Fig. 4 Configuration of type-II model.

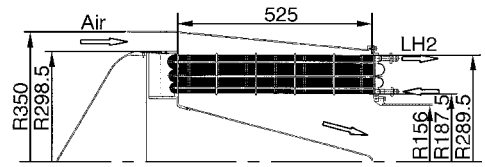

Fig. 5 Configuration of type-III model.

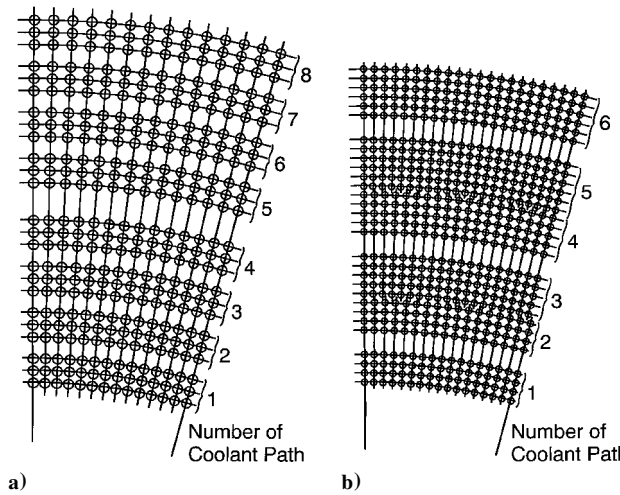

Fig. 6 Tube arrangement of a) type-I model and b) type-III model.

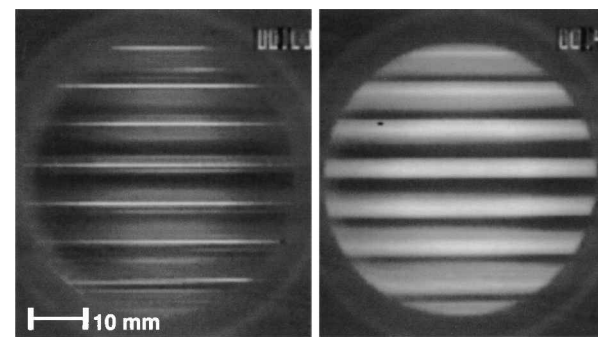

a) Before cooling **b) 15 s after cooling**

Fig. 7 Frost formation on outermost tubes (type I).

plates were turned to cross at right angles with tubes, which also could help easy fabrication. The reduction of pressure drop was attained by enlarging the inlet airflow area. Moreover, lip plates were equipped at outer tube assembly for uniform air admission.

As a result of these modifications, six test runs (280 s) were successfully conducted without trouble, and the pressure drop of airflow could be reduced by 30%. However, the heat transfer rates were still 15–20% smaller than the predicted values. This could be mainly due to the frost layer, although it is not so thick as to cause the additional pressure drop of airflow.

Type-III Model

The type-III model was designed for compactness and light weight in view of a future flying test.[5] This objective was achieved by using tubes with smaller diameter and arranging them closely, as shown in Fig. 6. In place of the lip plates, a tapered outer shell was adopted to get uniform admission of airflow. Moreover, the weight of the manifolds and structural components was thoroughly cut down based on a stress analysis. As a result of these improvements, the volume and the weight of this model could be considerably reduced without lowering its performance, as listed in Table 1.

This model was tested in 1998. The heat transfer rates of this model were better than those of previous models, although it was

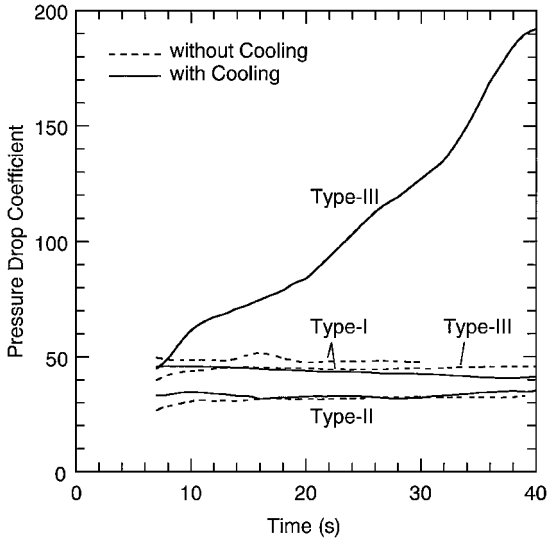

Fig. 8 Transition of pressure drop.

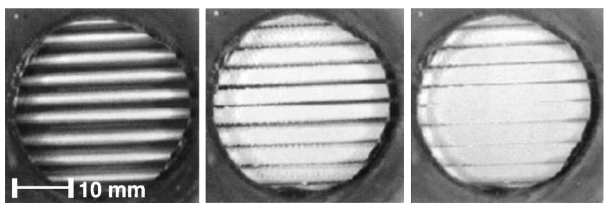

a) b) c)

Fig. 9 Frost formation on outermost tubes (type III): a) before cooling, b) 15 s after cooling, and c) 30 s after cooling.

still smaller than its expected value. However, the pressure drop of the airflow increased rapidly during the test run, as shown in Fig. 8. This was because the frost layer formed on the tube surfaces as shown in Fig. 9. Frost formation emerged only from this test because the tube gap of this model was smaller than that of the previous models, especially in the outermost rows, and the absolute humidity in these tests was much higher than that of the previous tests.

These test results indicated that a good understanding of the frosting effect is indispensable for further development of the precooler.

Study of Frost Formation

Frost formation on a heat exchanger has been investigated by many researchers.[6,7] However most of them were working on the heat exchanger of refrigerator or air-conditioning equipment, whose conditions such as cooling wall and air temperatures were much different from those of the precooler, as listed in Table 2. Therefore, the characteristics of the frost formation in the precooler were still uncertain. For that reason, an experimental study has been performed since 1998 to investigate the frost formation in a wide range of cooling wall and main flow temperatures by using a subscale heat exchanger model.

According to the results of a previous study,[8] it was found that the frost layer formed on the heat exchanger surface in a cryogenic state has a low density and a low thermal conductivity, and therefore it grows rapidly resulting in large resistance both to the heat transfer and to the airflow through the tubes. Therefore, the performance of such a cryogenic heat exchanger as precooler declines immediately by frost formation.

Frost formation could cause a catastrophic failure in an acceleration phase at low altitude of a space plane using the ATREX engine. During this period (about several tens to several hundreds of seconds), the operation of the engine cannot be stopped by the defrosting cycles as applied in the heat exchanger for refrigeration or air conditioning. Therefore, some particular measures against the frost formation are strongly desired for the precooler.

Table 2 Comparison of frosting condition

Parameter	Heat exchanger for refrigeration or air conditioning	Precooler for ATREX engine
Coolant	R-22, etc.	LH2
Cooling wall temperature, K	>240	>30
Air temperature, K	>240	>160
Airflow velocity, m/s	≈1	≈10
Running time	≈1 h	≈1 min

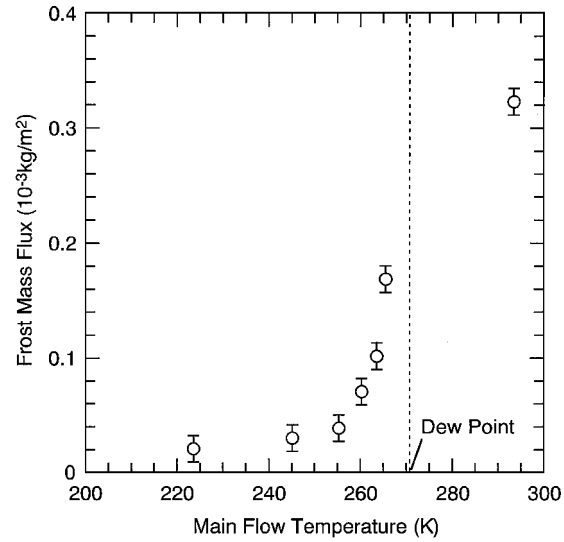

Fig. 10 Effect of main flow temperature on frost mass flux.

Measures Against Frost Formation

One solution to the problem proposed by Balepin et al. is liquid oxygen injection into the heat exchanger airflow inlet.[9] This method is based on the frost mass decreasing significantly if the air temperature is lower than the dew point. This was verified by the previous study,[8] as shown in Fig. 10. However, 0.1–0.3 kg of liquid oxygen is required to cool down 1 kg of atmospheric air sufficiently. Although the liquid oxygen works as an oxidizer, in some cases for the ATREX engine, such a large amount of the injection would cause decline of the total engine performance due to the weight of the equipment for the injection and the liquid oxygen itself.

For the mentioned problem, another innovative method will be proposed. A condensable gas, for instance, ethanol, is mixed at the upstream side of the precooler and is condensed or sublimated together with water vapor on the heat exchanger surface. If the condensable gas condenses or sublimates within the frost layer consisting of ice crystals and fills the space among them, the density and thermal conductivity of the frost layer would increase. Moreover, the thickness of the frost layer would decrease according to the lessening of the space in favorable case, and then both thermal and flow resistance of the frost layer would decrease. Consequently, it is expected to prevent the decline of the precooler performance caused by frost formation.

The condensable gas for this purpose should have the following properties. It is reasonably presumed that the same amount of the condensable gas is required to transfer onto the frosting surface as that of water vapor. Therefore, the saturated states should be similar to that of water vapor, and the diffusion coefficient should be as large as possible. Moreover, the melting point is recommended to be low because condensed liquid can easily seep into the frost layer. Examples of the condensable gas that satisfies these conditions are some hydrocarbons (toluene, *n*-heptane, ethylbenzene, *n*-octane, isooctane), lower alcohols (methanol, ethanol, propanol), ethyl acetate, and so on.

Experimental Setup and Procedure

To confirm the effectiveness of the method, an experimental program was carried out. Ethanol was selected as the condensable gas in the experiment. The experimental setup is shown schematically in Fig. 11. A half-open wind tunnel with a testing section of 84 × 84 mm was constructed and used.

Nitrogen gas was used for main flow instead of air to prevent liquid–air formation on the cooling wall. Ethanol was supplied into the dry nitrogen gas by the spray system (section A in Fig. 11) after being mixed with water at a given ratio. The gas temperature and humidity were adjusted after the droplets were entirely vaporized. The nitrogen gas containing water and ethanol vapor was induced into the test section by a centrifugal blower, whose power was controlled to keep the flow rate constant throughout each test.

Schematic drawing of the test heat-exchanger model is shown in Fig. 12. The test model was constructed from seven copper inner-finned tubes with 8 mm diameter arranged in a row right-angled to the main flow. Liquid nitrogen was supplied from a pressurized tank in section B (Fig. 11) and through small tubes inside the inner-finned tubes. The temperature of the tube wall was kept at about 90 K by boiling the liquid nitrogen.

Temperature and humidity of the main flow were measured at 100 mm upstream and 200 mm downstream of the test model. Flow velocity was measured by pitot tube at 100 mm upstream of the test model. The static pressure difference was measured between 100 mm upstream and 100 mm downstream of the test model. Temperature of the cooling wall was measured by thermocouples with 0.25 mm diam. Frost thickness was determined from the frosting surface recorded by using charge-coupled device cameras. Frost formation rate was obtained by weighing the frost scraped off from the tube surface at the certain time. The ratio of the ethanol in the frost layer was determined from the frost density, which was measured after melted.

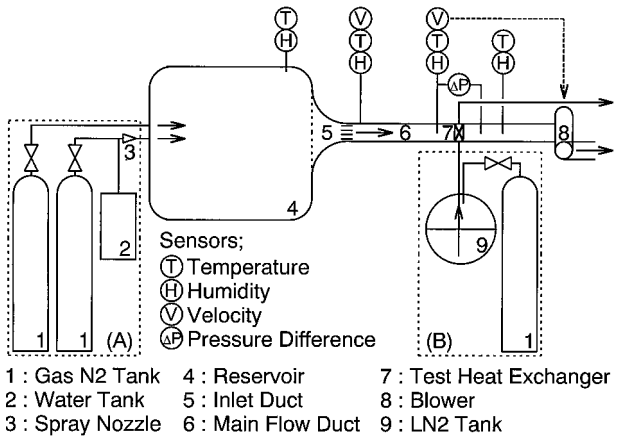

Fig. 11 Schematic of experimental apparatus.

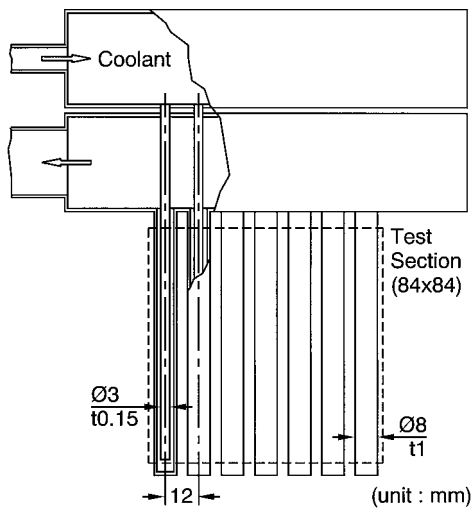

Fig. 12 Schematic of test heat exchanger.

Table 3 Test condition

Parameter	Value
Main flow velocity	3 ± 0.1 m/s
Main flow temperature	295 ± 3 K
Cooling wall temperature	90 ± 4 K
Water vapor mass fraction	3.2 ± 0.1 g/kg
Ethanol vapor mass fraction	0.0 – 8.4 ± 0.2 g/kg
Test duration	0 – 200 ± 1 s

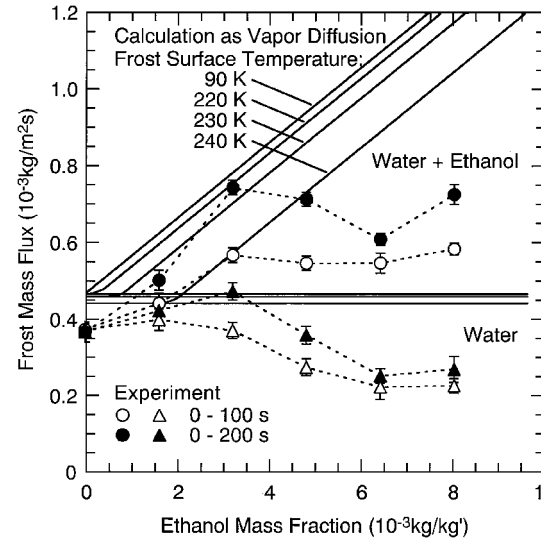

Fig. 13 Effect of ethanol mass fraction on frost mass flux.

Before the test, the model was covered to prevent early frost formation. Then the cooling process and the blow operation were started. Once the flow parameters and the cooling wall temperatures were uniform and stable, the model was uncovered, and the test started. After the test sequence was finished, the test model was removed from the test section, and the frost formed on the cooling tubes was scraped off into the sampling case and weighed. Test conditions are listed in Table 3.

Result: Frost Formation Rate and Composition

Average frost formation rates within 100- and 200-s test duration are shown in Fig. 13 and are determined from the weight of the frost layer formed on the front surface of the tubes at 100 and 200 s. Figure 14 shows ethanol mass ratio of the collected frost layer. Triangular symbols in Fig. 13 show the average water flux, which are determined from the total mass flux and the ethanol mass ratio. Lines in Figs. 13 and 14 are the values, calculated as the vapor mass flux by convective diffusion for different frost surface temperatures. The effect of frost surface variation, which might increase the mass flux by 20% at most, is neglected in this calculation.

If the ethanol mass fraction of the main flow is not too high, the measured mass flux increases with the ethanol mass fraction, which is roughly the same as the calculated value. However, as the ethanol mass fraction becomes higher, the measured mass flux does not increase in contrast to the calculated value. This discrepancy is attributed to the low frost surface temperature. When the frost surface temperature is quite low, the mass transfer process would be influenced by mist formation in the boundary layer and the transfer rate may decrease.[10] The result of the heat transfer rate mentioned later suggests that the frost surface temperature becomes lower if enough ethanol is added into the main flow.

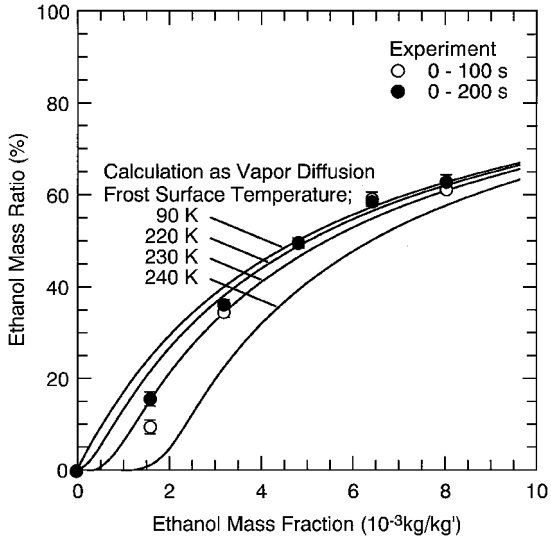

Fig. 14 Ethanol mass ratio of frost layer.

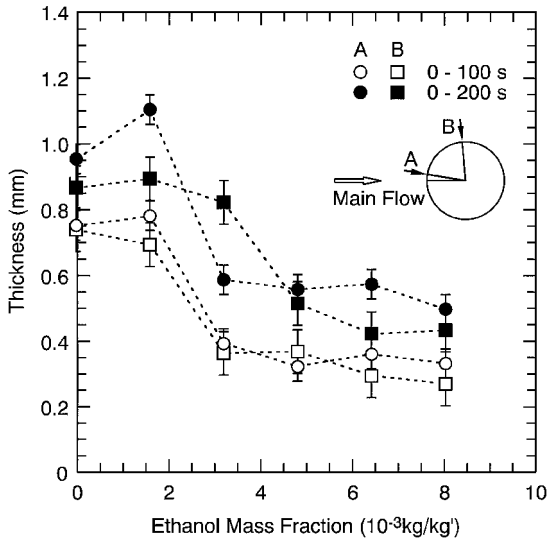

Fig. 15 Effect of ethanol mass fraction on frost thickness.

Result: Frost Thickness and Density

The frost thickness measured at the front and side of the tube is shown in Fig. 15. Figure 16 shows the averaged density of the frost layer formed on the front side of the tubes, which was determined from the mass and the thickness. The results show that the addition of ethanol makes the frost so dense that the thickness decreases even though the frost mass increases.

Result: Pressure Drop

The pressure drop coefficient, which is defined as pressure drop across the test heat-exchanger model divided by dynamic pressure of the main flow, is shown in Fig. 17 for different ethanol mass fractions. Figure 18 shows the relation between the frost thickness and the pressure drop coefficient. A line in the Fig. 18 shows the pressure drop across the tubes with equivalent diameters. The result shows that the pressure drop is strongly affected by the frost thickness. The addition of ethanol can restrain the increase of the pressure drop caused by frost formation.

Result: Heat Transfer

The heat flux, which is determined from the main flow velocity and its temperature difference between upstream and downstream of test heat-exchanger model, is shown in Fig. 19 for different ethanol mass fractions. The addition of ethanol can restrain the decrease of the heat flux caused by frost formation.

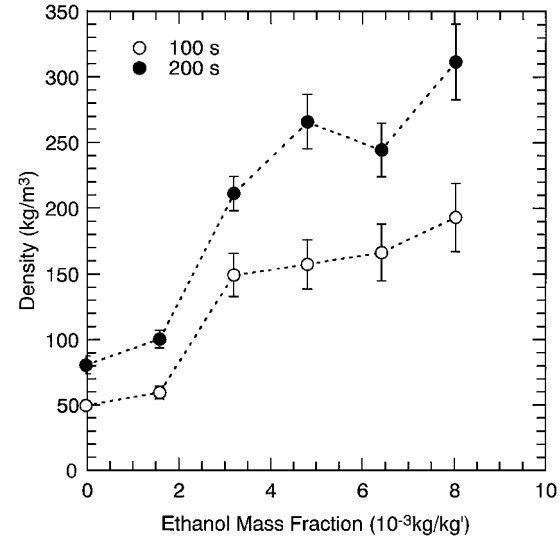

Fig. 16 Effect of ethanol mass fraction on frost density.

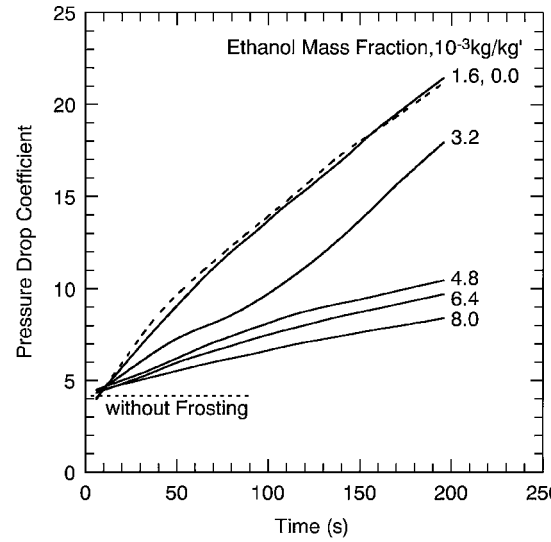

Fig. 17 Effect of ethanol mass fraction on pressure drop.

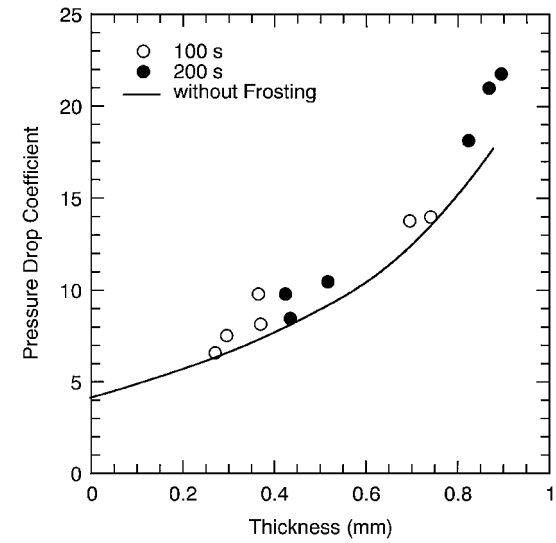

Fig. 18 Relation between pressure drop coefficient and frost thickness.

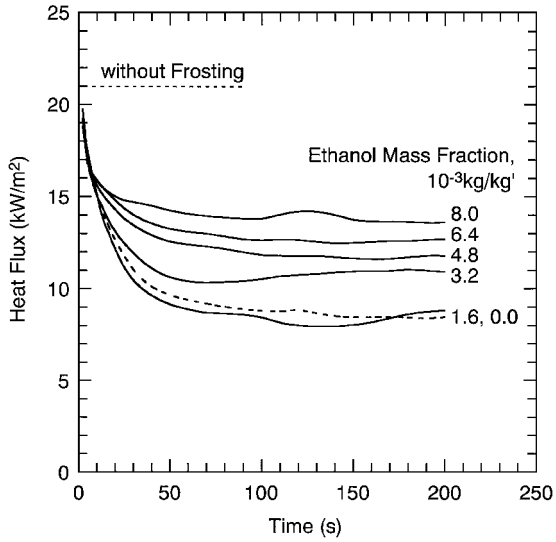

Fig. 19 Effect of ethanol mass fraction on heat flux.

Conclusion of Experiment

As a result of the experiment, the addition of ethanol into the main flow turned out to be effective method to restrain the decline of the precooler performance due to frost formation. This method requires just a small quantity of ethanol addition, as much as the water vapor contained in atmospheric air, which is about 1% of the air at sea level and much less at high altitude. The total mass of required ethanol estimated for a flight path of the ATREX engine (from sea level to 30-km altitude) is less than 3% of the fuel load. Therefore, the method is easily put to practical use at small cost in the performance.

Conclusion

A review of the development of three types of precooler models for the ATREX ground-test engine was given. The newest model precooler, type III, is much more compact and lighter weight than the former models without lowering its heat-exchange performance. In contrast, serious pressure drop of airflow was caused by frost formation. Therefore, frost formation in the precooler was an essential subject of investigation for further development. To improve the precooler performance under frosting conditions, a novel method of ethanol addition was proposed, and its effectiveness was confirmed by experiments with a subscale heat-exchanger model. The method will be applied in the next firing test of the ATREX engine installed with the type-III precooler model.

Acknowledgments

The precoolers for the ATREX engine ground-test model were developed in cooperation with Kawasaki Heavy Industries, Ltd. The development of the type-III model was supported by the New Energy and Industrial Technology Development Organization of the Ministry of International Trade and Industry of Japan.

References

[1]Tanatsugu, N., "Development Study on Air Turboramjet," *Developments in High-Speed-Vehicle Propulsion System*, edited by S. N. B. Murthy, Vol. 165, Progress in Astronautics and Aeronautics, AIAA, New York, 1996, pp. 259–331.

[2]Balepin, V. V., Tanatsugu, N., Sato, T., Mizutani, T., Hamabe, K., and Tomike, J., "Development Study of Precooling for ATREX Engine," *Proceedings of the Twelfth International Symposium on Air Breathing Engines*, Vol. 1, AIAA, Washington, DC, 1995, pp. 173–182.

[3]Tanatsugu, N., Sato, T., Naruo, Y., Kashiwagi, T., Mizutani, T., Monji, T., and Hamabe, K., "Development Study on ATREX Engine," International Astronautical Federation, IAF Paper 96-S.5.03, Oct. 1996.

[4]Harada, K., Yamauchi, H., Tanatsugu, N., Sato, T., Okabe, Y., Hamabe, K., Tomike, J., and Kazari, M., "Development Study on Precooler for ATREX Engine," *Advances in the Astronautical Sciences*, Vol. 96, 1997, pp. 251–257.

[5]Sato, T., Tanatsugu, N., Naruo, Y., Omi, J., Tomike, J., and Nishino, T., "Development Study on ATREX Engine," International Astronautical Federation, IAF Paper 98-S.5.01, Sept. 1998.

[6]O'Neal, D. L., and Tree, D. R., "A Review of Frost Formation in Simple Geometries," *American Society of Heating, Refrigerating and Air-Conditioning Engineers Transactions*, Vol. 91, No. 2A, 1985, pp. 267–281.

[7]Kondepudi, S. N., and O'Neal, D. L., "The Effect of Frost Growth on Extended Surface Heat Exchangers Performance—A Review," *American Society of Heating, Refrigerating and Air-Conditioning Engineers Transactions*, Vol. 93, No. 2, 1987, pp. 258–274.

[8]Harada, K., Yamauchi, H., Kessling, T., Tanatsugu, N., and Sato, T., "Experimental Study of Frost Formation on Cryogenic Heat Exchanger," *Proceedings of the Twenty-First International Symposium on Space Technology and Science*, Vol. 1, edited by K. Uesagi, 21st International Symposium on Space Technology and Science Publications Committee, Tokyo, 1998, pp. 153–158.

[9]Balepin, V. V., Maita, M., Tanatsugu, N., and Murthy, S. N. B., "Deep-Cooled Turbojet Augmented with Oxygen Cryojet for an SSTO Launch Vehicle," AIAA Paper 96-3036, July 1996.

[10]Holten, D. C., "A Study of Heat Mass Transfer to Uninsulated Liquid Oxygen Containers," *Advances in Cryogenic Engineering*, Vol. 6, 1961, pp. 199–508.